Basic mechanism for abrupt monsoon transitions

Anders Levermann [*] [†], **Jacob Schewe** [*] [†], **Vladimir Petoukhov** [*], **and Hermann Held** [*]

[*] Earth System Analysis, Potsdam Institute for Climate Impact Research, Potsdam, Germany, and [†] Institute of Physics, Potsdam University, Potsdam, Germany

Submitted to Proceedings of the National Academy of Sciences of the United States of America

Supporting Information

Monsoon regions and definitions

NCEP/NCAR reanalysis data was obtained from http://www.cdc.noaa.gov/ as 60-year monthly mean time series, starting January 1948. Heat flux and precipitation data are averaged over land in each monsoon region. ΔT is the difference between the average temperatures over land and ocean. Humidities q_L and q_O refer to the same land and ocean regions, respectively. The near-surface, landward zonal wind velocity W is averaged over a third region. All three regions are given in table 1 and illustrated in figures S1 and S2, together with the respective definitions of the monsoon season that are used for the temporal averages shown in figures 3 and 4. W is averaged vertically between 850hPa and 1000hPa. q_O is averaged vertically between 600hPa and 1000hPa. All other vertical averages are over the entire atmospheric column.

Robustness of R_C estimate

In order to determine the statistical stability of the estimate of the distribution of R_C, we proceeded in two steps. (1) From the time series' autocorrelation we decided to treat the time series of α and β as containing virtually no memory, i.e. values from different years can be treated as statistically independent. Note that this assumption does not contradict the existence of interannual to decadal variability that is forced externally. (2) Via bootstrapping we generated surrogate time series of length 60. From this time series ensemble we found that the standard deviation of mean and standard deviation of the R_C-distribution are one order of magnitude below the standard deviation of the shown distribution of R_C-estimates. Hence the red curves in figure 6 are already relatively robust estimates, in view of the simplicity of the model approach.

Structural sensitivity of conceptual model

In order to analyse the structural robustness of the governing equation [6] to inclusion of further physical processes we start from the non-dimensional forms of the unperturbed equations [1] and [3]

$$lp - w^2 + r = 0 \qquad \textbf{[S1]}$$

$$w(1-p) - p = 0 \qquad \textbf{[S2]}$$

using the same definitions of parameters l and r and non-dimensional variables w and p as in the main text. Note that the parameter l as computed from observations is of the order 10^4. Its qualitative influence on the solution structure can, however, already been seen for $l = 1$. Since 1 is the only other scale in the non-dimensional governing equation, we will use $l = 1$ as an example. Similarly we will show the qualitative influence of other paramters by setting them to 0.5 without claiming this to be an observed value. Note that for some cases the critical precipitation reduces and could in principle become zero or negative. This would change the model behaviour qualitatively. However this can only be the case when the corresponding process dominates the dynamics and is not merely a perturbation to the dynamics described in the core model. Non of the processes included eliminates the bifurcation for small parameter values. In this sense the model behaviour is robust.

Addition of evaporation. To our understanding, the strongest missing process is the effect of evaporation over land. In order to estimate the critical threshold of different monsoon systems we generalize the model by adding evaporation to the moisture budget (equation [3]). In the reanalysis data evaporation provides a very weak feedback within the dynamics and is well approximated by $P - E \approx \gamma P - E_O$, with region-specific constants E_0 and γ which is close to unity (figure S4). For this purpose we replace equation [S2] by $w(1-p) - (\gamma p - e)$ with $e \equiv E_0/(\beta q_O)$. This equation can also be derived from the approach by Hansen et al. [1] and an additional assumption of constant total soil moisture within a rainy season. We obtain

$$p = \frac{w+e}{w+\gamma} \qquad \textbf{[S3]}$$

Accordingly, the governing equation transforms to

$$w^3 + \gamma w^2 - (l+r)\,w - (el + \gamma r) = 0 \qquad \textbf{[S4]}$$

Both constant and precipitaton-dependent evaporation shift critical radiation to lower and critical precipitation towards higher values (figure S5). As in the minimal model set-up, the critical threshold can be computed analytically from

$$w_c\,(w_c+\gamma)^2 = (\gamma - e)\,l/2 \qquad \textbf{[S5]}$$

$$r_c = 3w_c^2 + 2\gamma w_c - l$$

By additional use of the evaporation time series $E(t)$ from NCEP/NCAR reanalysis, the parameter e can be computed.

$$e = E(t)/(\beta q_O(t)) \qquad \textbf{[S6]}$$

By assuming γ to be constant (taken from the regression in figure S4), the critical threshold of this generalized model can be computed (figure 6).

Addition of cloud-albedo feedback. Assuming that cloud-albedo over land increases with the atmospheric moisture content we add a term $-a' q_L$ to equation [1] where a' is a constant. Consequently the nondimensional heat equation is transformed into

$$(l-a)\,p - w^2 + r = 0 \qquad \textbf{[S7]}$$

where $a \equiv a' q_O \epsilon\alpha/\left(C_p\beta^2\right)$. The governing equation

$$w^3 + w^2 - (l + r - a)\,w - r = 0 \qquad \textbf{[S8]}$$

shows the same functional form with an effective shift of the original l-parameter towards lower values (figure S6). This reduces the significance of the moisture-advection feedback for the monsoon circulation by lowering the threshold precipitation value. On the other hand the threshold is reached at higher net radiation r_c.

Reserved for Publication Footnotes

Tab. S1: Regional definitions used for data analysis

Monsoon system	INDIA	BAY OF BENGAL	CHINA	W.AFRICA	N.AMERICA	AUSTRALIA
Land region	$70-90^\circ E$	$80-100^\circ E$	$100-110^\circ E$	$15^\circ W-10^\circ E$	$110-100^\circ W$	$120-150^\circ E$
	$5-30^\circ N$	$15-30^\circ N$	$25-30^\circ N$	$2-14^\circ N$	$20-30^\circ N$	$18-10^\circ S$
Ocean region	$65-78^\circ E$	$80-100^\circ E$	$80-100^\circ E$	$28^\circ W-10^\circ E$	$120-110^\circ W$	$100-130^\circ E$
	$5-30^\circ N$	$10-20^\circ N$	$10-20^\circ N$	$5^\circ S-14^\circ N$	$20-30^\circ N$	$10-0^\circ S$
Wind region	$65-78^\circ E$	$80-100^\circ E$	$90-105^\circ E$	$15^\circ W-10^\circ E$	$111-109^\circ W$	$100-130^\circ E$
	$5-30^\circ N$	$15-30^\circ N$	$15-25^\circ N$	$2-9^\circ N$	$20-30^\circ N$	$10^\circ S-0^\circ$
Monsoon season	JJA	JJA	JJA	JAS	JJA	JFM

Addition of constant equatorial easterlies. The effect of a constant inflow of moist air leads to an addition of a constant w_t to the winds in the heat balance and moisture balance equations

$$lp - w\left(w + w_t\right) + r = 0 \quad \textbf{[S9]}$$

$$\left(w + w_t\right)\left(1 - p\right) - p = 0 \quad \textbf{[S10]}$$

yielding the governing equation

$$w^3 + \left(2w_t + 1\right) w^2 - \left(l + r - w_t\left(w_t + 1\right)\right) w - \left(\left(1 + w_t\right) r + l w_t\right) = 0 \quad \textbf{[S11]}$$

and a shift of the critical threshold towards lower radiation and precipitation values (figure S7).

Addition of stabilizing radiative feedback. Adding a negative contribution $-\sigma' T_L$ to the heat balance may be used to parameterize a stabilizing temperature feedback due to changes in long wave radiation. This addition transforms the non-dimensional heat balance into

$$lp - \left(w + \sigma\right) w - \sigma t_O + r = 0 \quad \textbf{[S12]}$$

where $\sigma \equiv \sigma' / \left(C_p \beta\right)$ and $t_O \equiv T_O \alpha \epsilon / \beta$ is the nondimensional atmospheric temperature over the ocean. The resulting governing equation

$$w^3 + \left(\sigma + 1\right) w^2 - \left(l + r - \sigma\left(\sigma + 1\right)\right) w - \left(r + \sigma t_O\right) = 0 \quad \textbf{[S13]}$$

resembles the corresponding relation with additional trade winds (figure S8).

Addition of threshold for precipitation. Adding a threshold moisture value q_{th} to equation [4] above which precipitation is initiated does not change the governing equation after redefining $p \equiv P / \left(\left(q_O - q_{th}\right) \beta\right)$. It however changes the physical quantities. Critical precipitation then reduces to zero when the threshold value approaches q_O.

1. Hansen J, *et al.* (1983) Efficient three-dimensional global models for climate studies: Models I and II. *Monthly Weather Review* 111:609–662.

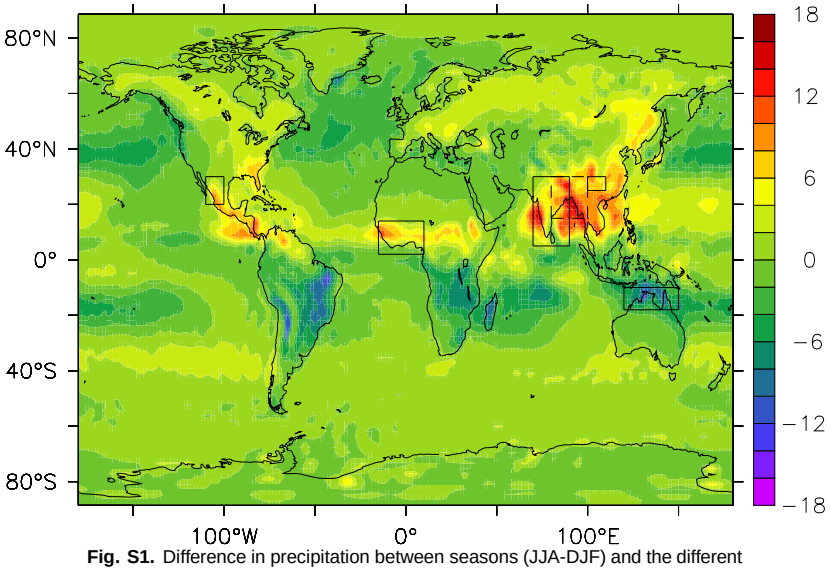

Fig. S1. Difference in precipitation between seasons (JJA-DJF) and the different monsoon regions studied (black boxes).

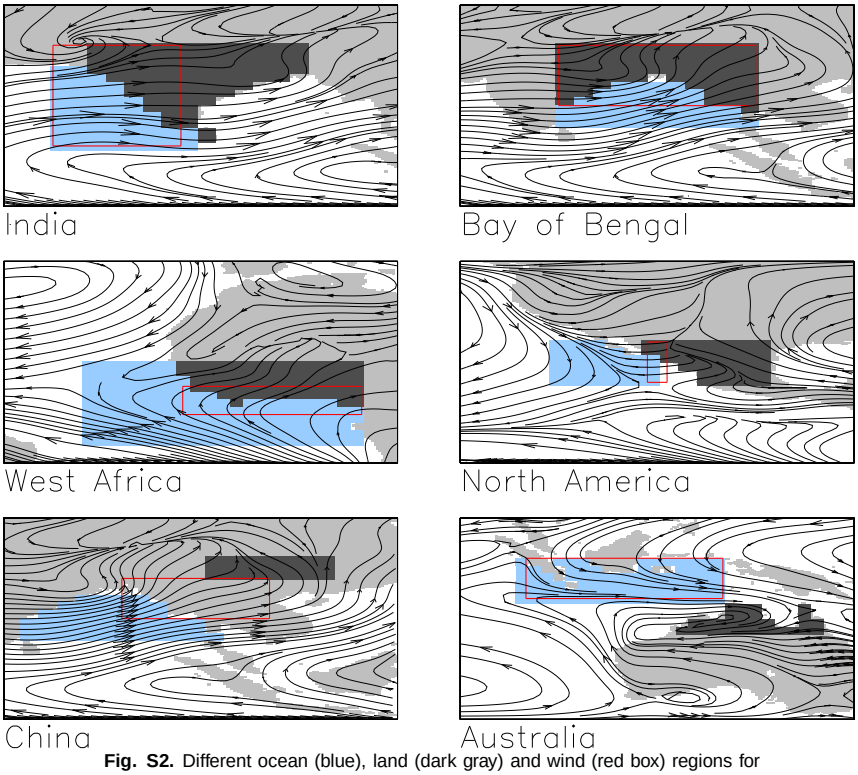

Fig. S2. Different ocean (blue), land (dark gray) and wind (red box) regions for the different monsoon systems as used for computation of the different quantities used to motivate the conceptual model. Flow lines represent summer winds connecting the ocean with the land region.

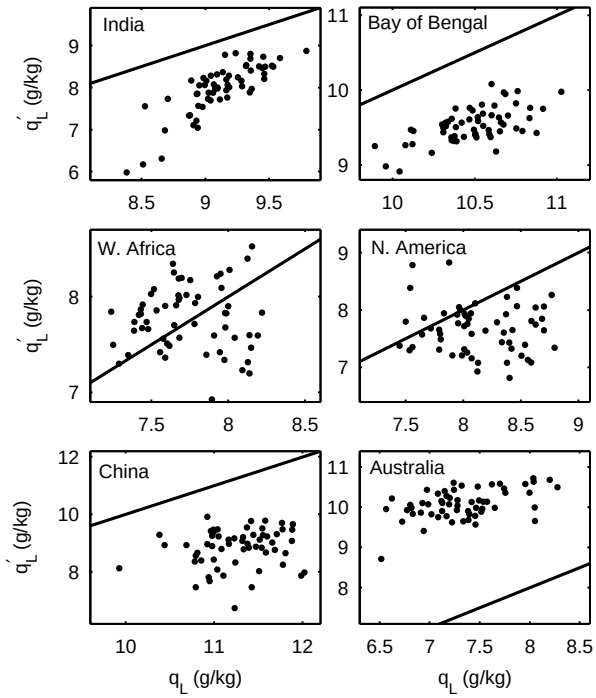

Fig. S3. Specific humidity q'_L over land as computed by the model from time series for precipitation, radiation, temperature difference and specific humidity over the ocean versus observed mean specific humidity over land q_L. The line gives the unit function $q'_L = q_L$

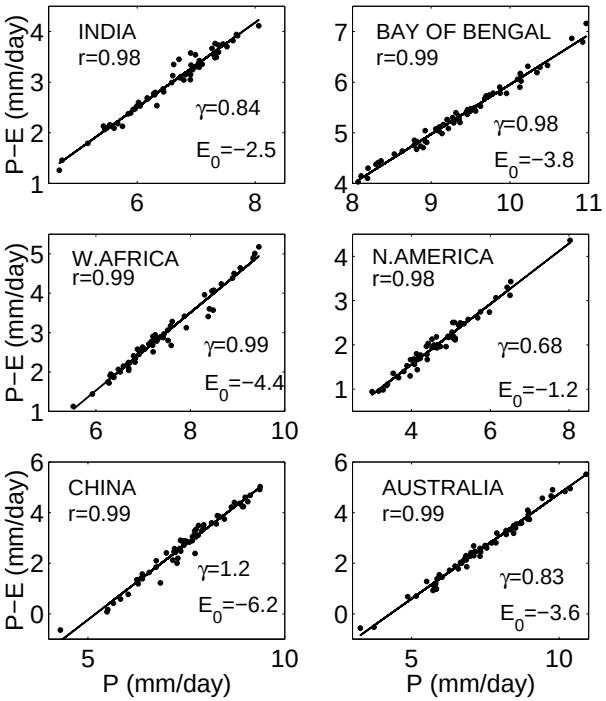

Fig. S4. Scaling of precipitation minus evaporation with precipitation in NCEP-NCAR reanalysis data.

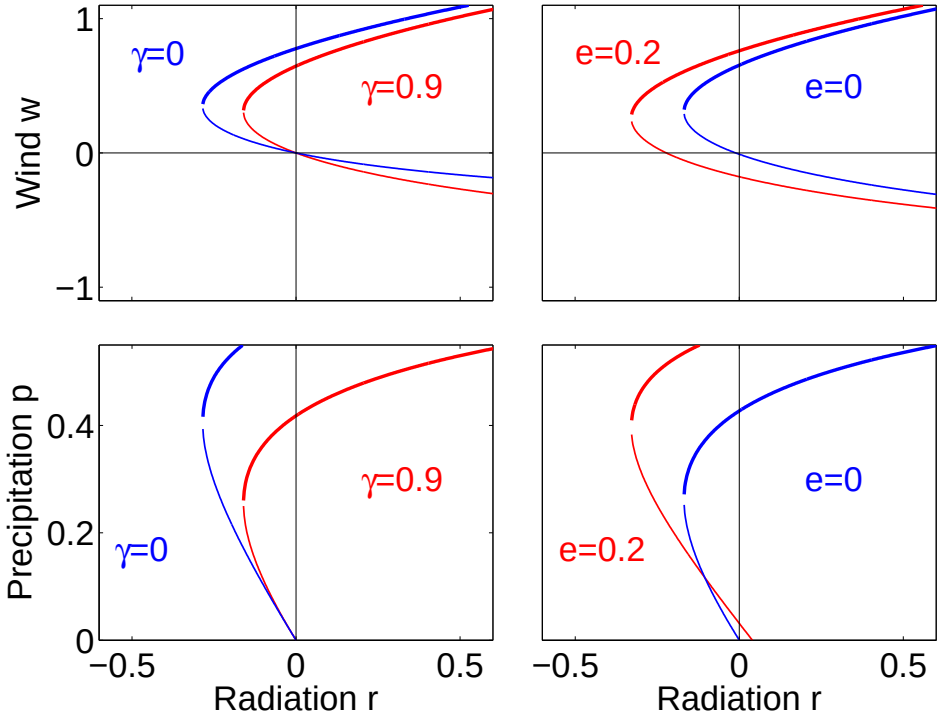

Fig. S5. Change in solution structure due to inclusion of evaporation. Left: constant offset $e = 0.2$ without linear dependence on precipitation $\gamma = 1$ (equation [S4]). Right: linearly dependent evaporation $\gamma = 0.9$ without constant offset $e = 0$.

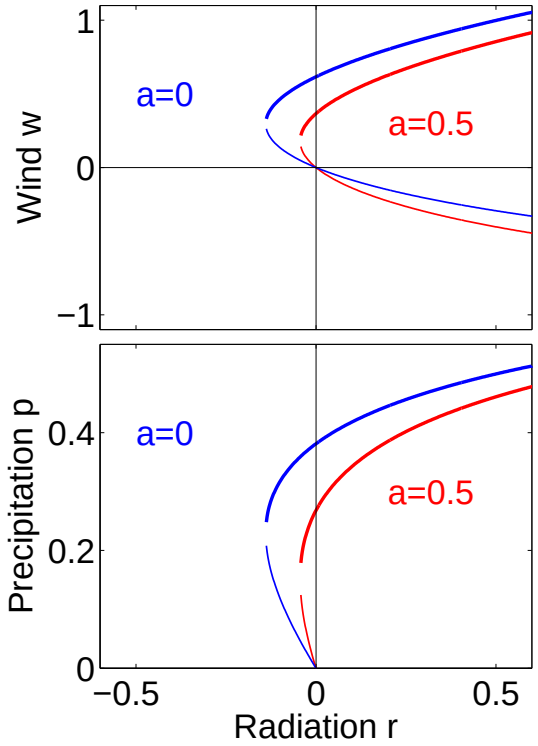

Fig. S6. Change in solution structure due to inclusion of the cloud-albedo feedback

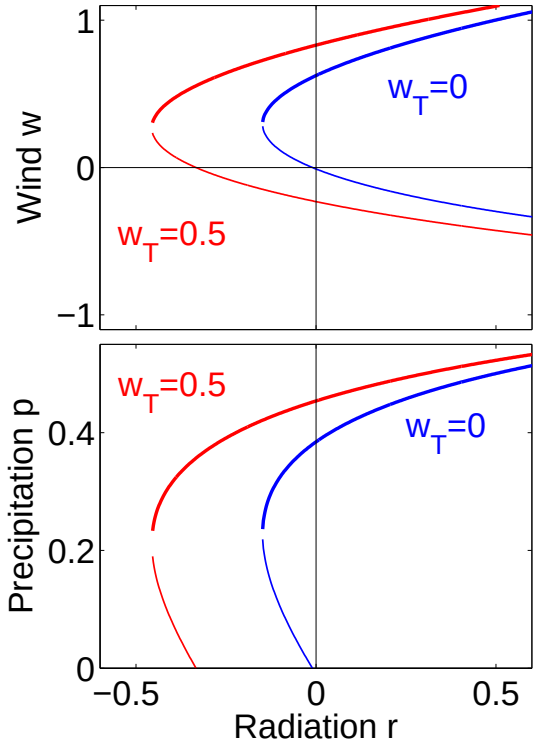

Fig. S7. Change in solution structure due to inclusion of an inflow of moisture and heat by constant trade winds

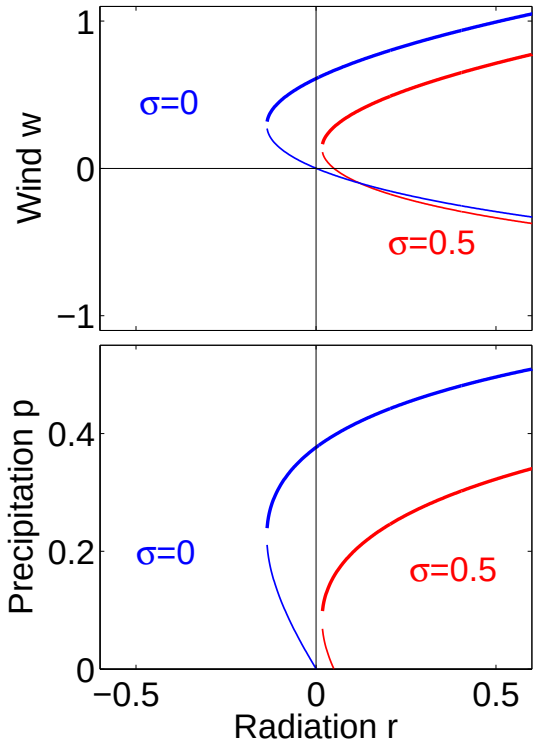

Fig. S8. Change in solution structure due to inclusion of a stabilizing long wave radiation feedback